

Antimitotic herbicides bind to an unidentified site on malarial parasite tubulin and block development of liver-stage *Plasmodium* parasites

Enda Dempsey^a, Miguel Prudêncio^b, Brian J. Fennell^{a,1}, Carina S. Gomes-Santos^b, James W. Barlow^c, Angus Bell^{a,*}

^a Department of Microbiology, School of Genetics & Microbiology, Moyné Institute of Preventive Medicine, Trinity College Dublin, Dublin 2, Ireland

^b Instituto de Medicina Molecular, Faculdade de Medicina, Universidade de Lisboa, Av. Prof. Egas Moniz, 1649-028 Lisboa, Portugal

^c Department of Pharmaceutical & Medicinal Chemistry, Royal College of Surgeons in Ireland, Stephen's Green, Dublin 2, Ireland

ARTICLE INFO

Article history:

Received 10 October 2012

Received in revised form 7 March 2013

Accepted 14 March 2013

Available online 21 March 2013

Keywords:

Malaria

Plasmodium

Tubulin

Microtubules

Antimalarial chemotherapy

ABSTRACT

Malarial parasites are exquisitely susceptible to a number of microtubule inhibitors but most of these compounds also affect human microtubules. Herbicides of the dinitroaniline and phosphorothioamide classes however affect some plant and protozoal cells but not mammalian ones. We have previously shown that these herbicides block schizogony in erythrocytic parasites of the most lethal human malaria, *Plasmodium falciparum*, disrupt their mitotic spindles, and bind selectively to parasite tubulin. Here we show for the first time that the antimitotic herbicides also block the development of malarial parasites in the liver stage. Structure-based design of novel antimalarial agents binding to tubulin at the herbicide site, which presumably exists on (some) parasite and plant tubulins but not mammalian ones, can therefore constitute an important transmission blocking approach. The nature of this binding site is controversial, with three overlapping but non-identical locations on α -tubulin proposed in the literature. We tested the validity of the three sites by (i) using site-directed mutagenesis to introduce six amino acid changes designed to occlude them, (ii) producing the resulting tubulins recombinantly in *Escherichia coli* and (iii) measuring the affinity of the herbicides amiprofosmethyl and oryzalin for these proteins in comparison with wild-type tubulins by fluorescence quenching. The changes had little or no effect, with dissociation constants (K_d) no more than 1.3-fold (amiprofosmethyl) or 1.6-fold (oryzalin) higher than wild-type. We conclude that the herbicides impair *Plasmodium* liver stage as well as blood stage development but that the location of their binding site on malarial parasite tubulin remains to be proven.

© 2013 Elsevier B.V. All rights reserved.

1. Introduction

The ability of microtubules (MT) to assemble and disassemble reversibly and in a non-equilibrium fashion is key to their many functions in eukaryotic cells [1]. This dynamic instability is frequently targeted by tubulin-binding MT poisons, as small perturbations in the process can be lethal [2]. This is especially true for fast-dividing cells, as mitotic division is exquisitely susceptible to disruption of the microtubular spindle. As a result, tubulin-binding

compounds have proven to be successful anti-cancer agents [3,4]. However, they have also proven effective against slower growing cells, such as helminth parasites [4,5].

The use of MT inhibitors as drugs for protozoal infections has been more limited, but a number of MT inhibitors have potent activity on a range of protozoal pathogens [4]. The malarial parasite *Plasmodium* is highly susceptible to a number of MT inhibitors, with 50% inhibitory concentrations (IC₅₀) on cultured, asexual, blood-stage parasites of the most lethal malaria species *P. falciparum* as low as 100 pM [6], well below those of most antimalarial drugs in use. The major target for MT inhibitors in this parasite stage appears to be the series of mitotic divisions that occur in the schizont, just before formation and release of new merozoites [7]. There have also been reports of effects of MT inhibitors on invasion of erythrocytes by merozoites [8] and on the development of pre-sexual blood stages (gametocytes) [9]. As mitotic inhibitors, they might also be expected to be effective on the liver stage that precedes the blood stage, where multiple divisions occur before the release of the first merozoites, but this has never been reported. This issue is

Abbreviations: APM, amiprofosmethyl; BSA, bovine serum albumin; GFP, green fluorescent protein; MBP, *Escherichia coli* maltose-binding protein; MCAC, metal-chelate affinity chromatography; MT, microtubule; PIPES, 1,4-piperazinediethanesulphonic acid; SDS-PAGE, sodium dodecyl sulphate-polyacrylamide gel electrophoresis.

* Corresponding author. Tel.: +353 1896 1414; fax: +353 1679 9294.

E-mail address: abell@tcd.ie (A. Bell).

¹ Present address: Global Biotherapeutic Technologies, Pfizer, Grangecastle, Dublin 22, Ireland.

potentially important because of the paucity of proven inhibitors of liver-stage parasites [10,11].

Unfortunately, blood-stage *Plasmodium* parasites are no more susceptible than mammalian cells to the classical MT inhibitors colchicine, vinblastine and taxol nor to other anticancer agents tested to date [9,12]. This lack of selectivity has so far precluded the development of novel antimalarial drugs from these compounds. The dinitroaniline and phosphorothioamidate herbicide classes are however an exception in that they are active against *Plasmodium* as well as certain other protozoa, fungi and plants, but ineffective against mammalian cells [13,14]. This distinction appears to be based at least in part on differences in binding affinities for the tubulins of these different organisms. Like colchicine, vinblastine and taxol, these compounds are known to bind to tubulin, but their binding sites (or site, as the two classes may bind in the same location [15]) have so far not been established.

Purified tubulins from a number of cell types have been used to measure the binding affinities of a range of MT inhibitors and the effects of these inhibitors on MT assembly and disassembly [16]. The ability to purify tubulin directly from a cell is however largely dependent upon its initial concentration, especially because purification strategies usually rely on cycles of assembly and disassembly of MT from tubulin in cell extracts, and this requires a minimum 'critical concentration' of tubulin for success [17]. As a result, a recombinant strategy has been adopted for tubulin-poor organisms [7,18–28], including *Plasmodium*, in which tubulin constitutes <1% of cellular protein [4]. Despite the complex chaperone machinery necessary for tubulin folding in intact cells [29], several groups have generated recombinant tubulins from bacterial hosts that are capable of ligand binding, recognition by conformation-dependent antibodies and in some cases assembly and disassembly [7,18–27,30–32]. Blood-stage *P. falciparum* are known to produce two α -tubulins, with α I-tubulin predominating in asexual parasites and α II-tubulin in gametocytes, but only one β -tubulin [4]. We previously reported the recombinant production of soluble *P. falciparum* tubulins in *E. coli* as fusions to *E. coli* maltose-binding protein (MBP) [7]. These tubulins could be bound by a radiolabelled version of the dinitroaniline herbicide trifluralin. Although binding to the tubulins was much higher than to MBP alone or to an irrelevant protein, it was not possible, using this system, to measure the affinities of trifluralin for the α - and β -tubulin subunits. Moreover, the MBP-tubulins were not assembly competent when combined together, possibly because of the bulky (42-kDa) MBP tag.

In this paper we have adapted the MBP-tubulin system to measure the affinities of two tubulin-binding herbicides for *P. falciparum* tubulin. We have also addressed the question of the binding site of the herbicides. At least three overlapping but distinct sites of dinitroaniline binding on α -tubulins of different species have been proposed in the literature [33–37]. These putative sites were proposed using *in silico* modelling and were based around known tubulin mutations that confer resistance to the herbicides. To date, only one study has used altered tubulin from the ciliate *Tetrahymena thermophila* in an attempt to validate one of these sites experimentally [38]. However, it is still not known whether any of the proposed sites is applicable to *Plasmodium*. We therefore specifically engineered α I-tubulin with novel amino acids and measured herbicide-binding affinity in order to validate one or other of the putative sites. We were unable to find evidence to support any of the sites in *P. falciparum* tubulin and believe that the herbicides more than likely bind at a novel site yet to be determined. Finally, we demonstrate here the activity of tubulin-binding herbicides on liver-stage *Plasmodium* parasites, the first report of MT inhibitors active on this stage of the parasite's life cycle.

2. Materials and methods

2.1. Reagents and plasmids

All chemicals and reagents were from Sigma–Aldrich (Dublin, Ireland) and were of analytical grade unless otherwise stated. Vinblastine, oryzalin and amiprofosmethyl (APM) (Fluka Chemie AG, Buchs, Switzerland) were all dissolved in dimethylsulphoxide. Primers were synthesized by IDT DNA Technology Inc. (Coralville, IA, USA). The pMAL-c2g (New England Biolabs, Hertfordshire, UK) vector was used for the majority of the cloning work. Recombinant plasmids were transformed into *E. coli* strains XL-1 Blue (Stratagene, CA, USA) and TB1 (New England Biolabs). Bovine brain tubulin (α/β) was obtained from Cytoskeleton (Denver, CO, USA).

2.2. PCR amplification, cloning and expression

The *P. falciparum* 3D7 α I- and β -tubulin were previously cloned into the pMAL-c2x vector [7]. These genes were sub-cloned into the pMAL-c2g vector using primers listed in Supplementary Table S1.

A "Hotstart" PCR was done using 0.5 μ M primer, \sim 100 ng DNA template, 2 mM dNTPs (Roche), 0.5 mM MgCl₂ (Promega), 1 unit *Pfu Turbo*[®] DNA polymerase (Stratagene, La Jolla, California, USA) and *Pfu Turbo*[®] buffer (Stratagene) in a 50- μ l reaction volume with a Techne TC-300 (Techne, Burlington, NJ, USA) thermocycler. The programme used for the PCR was: denaturation at 95 °C for 3 min; followed by 28 cycles of 95 °C for 30 s, annealing at 55 °C for 1 min and extension at 72 °C for 3 min; with a final extension at 72 °C for 7 min. The amplified fragments were separated on 1% agarose gels, excised and purified using a High Pure[®] PCR kit (Promega). The fragments were cloned into the pMAL-c2g vector using T4 DNA ligase (Roche Diagnostics Ltd., Lewes, East Sussex, UK) and transformed into CaCl₂-competent XL-1 Blue cells by a heat shock method [39]. Clones containing the construct of interest were identified by an increase in plasmid size using agarose gel electrophoresis and confirmed by DNA sequencing.

Nucleotide changes were introduced into the α I-tubulin gene by inverse PCR using the same conditions as above with the following exceptions. The programme used for the PCR was: denaturation at 95 °C for 3 min; followed by 28 cycles of 95 °C for 30 s, annealing at 55 °C for 1 min and extension at 72 °C for 9 min; with a final extension at 72 °C for 10 min. One unit of *DpnI* (NEB) was added to the PCR reaction and incubated at 37 °C for 3 h. The sample was cleaned up using a High Pure[®] PCR kit and transformed into XL-1 Blue cells as previously described.

The C-terminal His₆-tag encoding region was inserted into the tubulin genes using a modified inverse PCR strategy. This was done using 1 unit of KAPA HiFi[®] DNA polymerase (Kapa Biosystems, MA, USA), 0.3 μ M primer and 50 ng DNA template in a 25- μ l reaction volume using a Techne TC-300 thermocycler. The programme used for the PCR was: 95 °C for 3 min, followed by 30 cycles of 95 °C for 30 s, annealing at 60 °C for 20 s and extension at 72 °C for 5 min; with a final extension at 72 °C for 10 min. The sample was purified using a High Pure[®] PCR kit and digested with 1 unit of *DpnI* (NEB) and 1 unit of *XhoI*. The DNA was purified with a High Pure[®] PCR kit, ligated with T4 DNA ligase and transformed into XL-1 Blue cells as previously described.

2.3. Production and purification of recombinant proteins

The MBP-tagged tubulin fusion proteins were generated as previously described [7]. The MBP- and His₆-tagged tubulin fusions were also partially purified using a metal chelate affinity column and then subsequently purified on an amylose column.

Briefly, the recombinant proteins were produced by inoculating L-broth/ampicillin (100 µg/ml) in baffled flasks with overnight cultures of the strain of *E. coli* harbouring the construct of interest, and growing at 37 °C with agitation at 200 rpm to an $A_{600} \sim 0.5$. Recombinant gene expression was induced by the addition of 0.1 mM isopropyl-β-D-thiogalactopyranoside (Melford Laboratories, UK) and the culture was incubated for a further 1–3 h. Cells were harvested by centrifugation at $10,000 \times g$ for 5 min at 4 °C and were stored at –20 °C until required. The cells were resuspended in MCAC-0 buffer (20 mM Tris-HCl, 200 mM NaCl, pH 7.4) supplemented with Complete Mini EDTA-free protease inhibitor tablets (Roche) and were lysed by 2–3 passages through a pre-cooled French pressure cell at 2000 psi. Following clarification of the lysate by centrifugation at $40,000 \times g$ in a Sorvall RC50 Plus centrifuge using a SS-34 rotor for 1 h at 4 °C, the His₆-containing fusion proteins were purified from the soluble fraction on a Ni²⁺-loaded metal affinity column. The soluble fraction was loaded at 1 ml/min, washed with 20 column volumes of MCAC-60 buffer (MCAC-0 buffer supplemented with 60 mM imidazole) and eluted with 20 column volumes MCAC-150 buffer (MCAC-0 buffer supplemented with 150 mM imidazole). The eluate was loaded onto an amylose resin (NEB) at 1 ml/min, washed with 20 column volumes of amylose buffer (20 mM Tris-HCl, 200 mM NaCl, 1 mM EDTA pH 7.4) and eluted with elution buffer (amylose buffer supplemented with 10 mM maltose). The eluate was concentrated by ultra-filtration through Amicon centrifugal filter devices (Millipore) and the purity assessed by sodium dodecyl sulphate-polyacrylamide gel electrophoresis (SDS-PAGE). Protein concentration was determined using the assay of Bradford with bovine serum albumin (BSA) as the standard.

2.4. Co-sedimentation of the tubulin fusions with bovine tubulin

Decreasing concentrations of bovine tubulin (24 µM, 16 µM and 12 µM) were mixed with increasing concentrations of tubulin fusion protein (12 µM, 16 µM and 18 µM) so that the monomer ratio was 1:1, 1:2 and 1:3 respectively. The samples were made up as follows: bovine tubulin (12–24 µM), tubulin fusion protein (12–18 µM), GTP (2 mM), taxol (30 µM) 2-mercaptoethanol (1 mM) and GPEMG buffer (1 mM GTP, 80 mM 1,4-piperazinediethanesulphonic acid [PIPES]-NaOH, pH 6.9, 1 mM EGTA, 1 mM MgCl₂, 10% [v/v] glycerol). Taxol and 2-mercaptoethanol were not always included. BSA and purified MBP were used in place of the tubulin fusions as controls. Vinblastine (20 µM) was used in place of taxol to inhibit MT formation. The samples were incubated on ice for 30 min and then transferred to a 37 °C water bath for 1 h. Afterwards, the samples were overlaid on a pre-warmed (~37 °C) 60% (v/v) glycerol cushion in PEM buffer (80 mM PIPES-NaOH, pH 6.9, 1 mM EGTA, 1 mM MgCl₂) in sterile microcentrifuge tubes. MT were sedimented by the method of Kumar [40] through a glycerol cushion by centrifugation at $40,000 \times g$ at 37 °C in a Sorvall RC50 Plus centrifuge using a SS-34 rotor with specially outfitted Sorvall 408 adapter cones. Supernatant and cushion fractions were transferred to new microcentrifuge tubes containing equal volumes of 2× SDS-PAGE loading buffer (0.125 M Tris-HCl, pH 6.8, 2.3% (v/v) SDS, 10% (v/v) glycerol, 10% (v/v) 2-mercaptoethanol and 0.009% (w/v) bromophenol blue) and boiled for 10 min at 100 °C. The sedimented fraction was carefully rinsed using warm GPEMG buffer and re-centrifuged at $40,000 \times g$, 37 °C for 10 min. This wash step was repeated 2–3 times. The rinsed, sedimented fraction was resuspended in GPEMG buffer and 2× loading buffer and boiled at 100 °C for 10 min also. Equal quantities of protein sample were resolved by SDS-PAGE and densitometry was performed using the Quantity One® software (Bio-Rad Laboratories Inc., CA, USA).

2.5. Protein affinity assay using the tubulin fusion proteins

The affinity of the tubulin fusions for other proteins was determined by their ability to retain the protein(s) after a purification step using a metal affinity column. Sixteen µM of non-His₆-tagged proteins (MBP-α-tubulin or MBP), were added alone or with 16 µM of MBP-β-tubulin-His₆ to 1 mM GTP and GPEMG buffer in a final volume of 300 µl. MBP-β-tubulin-His₆ was pre-incubated with 1 mM 2-mercaptoethanol before being mixed with the other sample components (final 2-mercaptoethanol concentration 0.25 µM). The samples were incubated on ice for 30 min, in a 37 °C water bath for 30 min and then on ice for 30 min. Nine hundred µl of cold MCAC-0 were added to the sample and it was then loaded onto a 1-ml Ni²⁺-chelate column at a rate of 1 ml/min. The column was washed with exactly 6 ml MCAC-0, 6 ml MCAC-60 and 6 ml MCAC-500 (MCAC-0 supplemented with 500 mM imidazole). The eluate (4.5 ml) was concentrated to exactly 50 µl, mixed with 2× SDS loading buffer and boiled for 10 min at 100 °C before being resolved by SDS-PAGE.

2.6. Gel electrophoresis, western blotting and densitometry

SDS-PAGE and western immunoblotting were done by standard methods as described previously [41]. Bands on gels were quantified using densitometry software Quantity-One (BioRad). Known protein concentrations were used as standards to quantify the unknown protein amounts. Bovine brain tubulin was separated on a modified SDS-PAGE using the procedure outlined by Banerjee et al. [42].

2.7. Alignments and modelling

Multiple sequence alignments were performed using the ClustalW program (<http://www.ebi.ac.uk/Tools/msa/clustalw2/>). Three-dimensional structures of αI-tubulin were obtained using the Molecular Operating Environment program (MOE 2008.10 release of Chemical Computing Group Inc., Quebec, Canada) with the assistance of C. Flood (School of Biochemistry & Immunology, Trinity College Dublin) to create homology models using as a template the *Bos taurus* α/β-tubulin dimer (PDB accession 1tub [43]) which has a completely resolved N-loop structure.

2.8. Fluorescence measurements by fluorescence spectroscopy

Tubulin or tryptophan samples were prepared in MME buffer (0.1 M 2-(N-morpholino)ethanesulphonic acid pH 6.9, 1 mM MgCl₂ and 1 mM EGTA). Tubulin samples had a final concentration of either 0.15 µM for the mixture of MBP-α/β-tubulin or 0.3 µM for the monomer alone. The tryptophan samples had a final concentration of 3.6 µM which corresponds to molar amount of tryptophans of the tubulin samples. Five µl of tubulin ligand (APM or oryzalin with a concentration of 0–20 mM) were added to the sample (final volume 500 µl). The sample was incubated at 37 °C for 5 min, then transferred to a thoroughly cleaned luminescence cuvette (Perkin Elmer, Waltham, MA, USA) and read using a spectrofluorimeter (Perkin Elmer LS-50B). The excitation and emission wavelengths were 280 nm and 300–400 nm respectively and both had a slit width of 4 nm. The absorbance of the sample was measured using a spectrophotometer (Shimadzu Scientific Instruments Inc., MD, USA). The sample was scanned every 0.5 nm from 280–400 nm. Inner filter effects were corrected for by using the Lakowicz equation, $F_{\text{corr}} = F_{\text{obs}} \text{antilog}[(A_{\text{ex}} + A_{\text{em}})/2]$ (where F_{corr} is corrected fluorescence, F_{obs} is observed fluorescence, A_{ex} is absorbance at the excitation wavelength and A_{em} is absorbance at the emission wavelength) [44]. In some cases, inner filter effects were corrected by measuring the quenching of N-acetyl-L-tryptophanamide (3.6 µM)

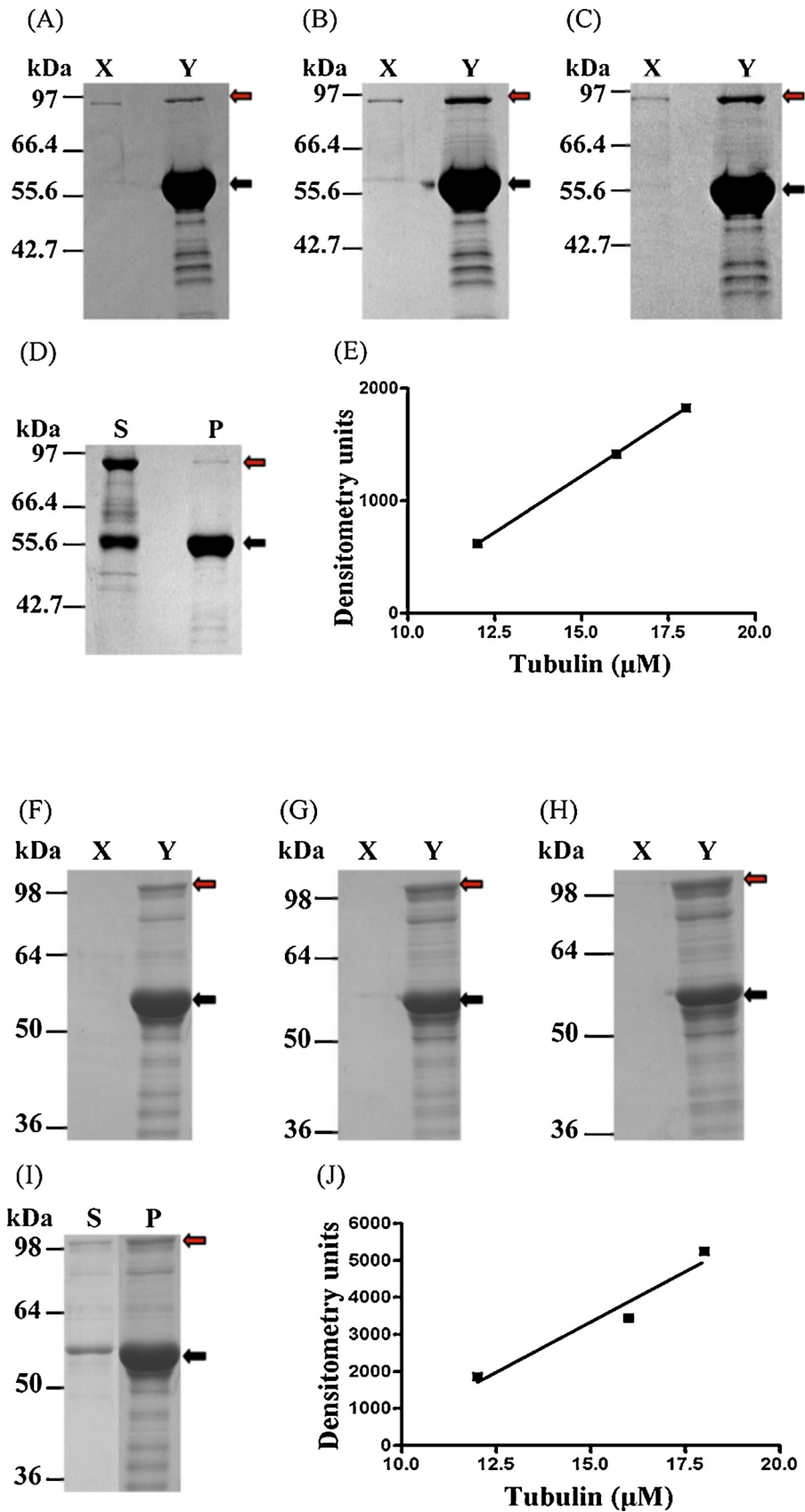


Fig. 1. Co-sedimentation of MBP-tubulins and bovine brain tubulin. Various concentrations of MBP- α -tubulin or MBP- β -tubulin, in the presence or absence of bovine brain tubulin, were incubated at 37 °C in the presence or absence of 30 μ M taxol and centrifuged through a glycerol cushion. The concentrations used were: (A) ~24 μ M bovine tubulin + 12 μ M MBP- α -tubulin; (B) ~16 μ M bovine tubulin + 16 μ M MBP- α -tubulin; (C) ~12 μ M bovine tubulin + 18 μ M MBP- α -tubulin; (F) ~24 μ M bovine tubulin + 12 μ M MBP- β -tubulin; (G) ~16 μ M bovine tubulin + 16 μ M MBP- β -tubulin; (H) ~12 μ M bovine tubulin + 18 μ M MBP- β -tubulin. The resulting pellets were resuspended in SDS-loading buffer and equal proportions from the pellet fractions of the control (MBP-tubulin fusion alone) (X) and bovine brain tubulin + MBP-tubulin mixture (Y) were

in the presence of the ligands. The dissociation constant (K_d) was determined using the following equation originally described by Acharya et al.: $F_{\max}/(F_0 - F) = 1 + K_d/L_f$, where L_f represents the free ligand equilibrium concentration in the reaction mixture and was determined by $L_f = C - X [Y]$ [45]. C represents the total concentration of ligand in the sample and Y is the molar concentration of ligand-binding sites. One high affinity binding site was assumed for all the calculations. The fraction of binding sites (X) occupied by a ligand were determined using the equation $X = (F_0 - F)/F_{\max}$, where F is the corrected fluorescence intensity of tubulin in the absence of a ligand, F_0 is the tubulin fluorescence in the presence of a ligand and F_{\max} was calculated by plotting $1/(F_0 - F)$ vs $1/[ligand]$ and extrapolating $1/[ligand]$ to zero.

2.9. Measurement of susceptibility of liver-stage parasites

To assess the effects of APM and oryzalin on liver stage *Plasmodium* infection in culture, Huh7 cells, a human hepatoma cell line, were treated with defined amounts of each inhibitor and infected with luciferase-expressing or green fluorescent protein (GFP)-expressing *P. berghei* parasites, freshly extracted from the salivary glands of infected *Anopheles* mosquitoes. Solvent-treated infected cells were used as controls. Infection loads were measured 48 h after infection by bioluminescence readings or flow cytometry, as previously described [46,47]. Briefly, luminescence measurements were carried out on infected cell lysates following addition of the luciferin substrate and flow cytometry analysis was performed on cells collected by trypsinization and resuspended in 2% fetal calf serum in PBS. Cells intended for luminescence measurements were infected with 10,000 sporozoites on 96-well plates and cells intended for flow cytometry analysis were infected with 30,000 sporozoites on 24-well plates. Inhibitors were added to the cells 1 h prior to sporozoite addition, for evaluation of their effect on overall infection, or 2 h after addition of sporozoites for evaluation of their effect on post-invasion parasite development. For microscopic observations, cells on glass coverslips were infected with 30,000 sporozoites on 24-well plates. Cells were fixed 48 h after infection with ice-cold methanol and stained with the 2E6 antibody (1/300 dilution) against the parasite's Hsp70, affinity-purified anti-*P. falciparum* β -tubulin antibody (1/50 dilution) (41) and the nuclear dye diaminophenylindole (DAPI). Anti-mouse Ig-AlexaFluor 594 and anti-rabbit Ig-AlexaFluor 488 (both at 1/400 dilution) were used as secondary antibodies for detection of the parasite's Hsp70 and MT, respectively. Infected cells were imaged on a Zeiss LSM 510 META confocal microscope (Zeiss, Oberkochen, Germany).

3. Results

3.1. Assessment of functionality of MBP-tagged tubulins

In a previous study [7], we used recombinant *P. falciparum* tubulins fused at their N-termini to MBP in order to obtain usable quantities of soluble tubulin from this organism. Recombinant approaches to tubulin production have been questioned on the grounds that if the proteins cannot be shown to be assembly competent, they may be improperly or incompletely folded and data obtained on ligand affinity, for example, may be misleading [38]. Combinations of α - and β -tubulins can form MT *in vitro* in the absence of other proteins under what are called 'assembly promoting' conditions. The MBP-tubulins together proved unable to form

MT but this was not unexpected given the presence of the bulky MBP tags on both subunits. We believed that the MBP-attached tubulins were likely to be correctly folded on the basis of (i) their high solubility, compared with the insolubility of untagged *P. falciparum* tubulins and (ii) their ability to ligate [14 C] trifluralin, whereas neither MBP alone nor bovine tubulins could do this [7]. Nonetheless, assembly competence remains the 'gold standard' for assessing tubulin functionality. Therefore, before developing a quantitative ligand binding assay for *P. falciparum* tubulins using the MBP-fusion proteins, we sought further reassurance of their correct folding. Extensive efforts to produce significant quantities of soluble untagged tubulin, to cleave the MBP tag or to co-express the two proteins had proved fruitless (data not shown).

In view of the high amino acid sequence conservation of tubulins and the ability of tubulins from different species to co-assemble [20,48,49], we attempted co-assembly of MBP-tubulins with bovine brain tubulin using a previously described co-sedimentation assay [50]. In this assay, MT are allowed to form in assembly promoting conditions before being sedimented by high-speed centrifugation (Fig. 1). Unassembled tubulin is found in the supernatant. The supernatant and pellet fractions were resolved by SDS-PAGE and densitometry was used to determine the relative amounts of tubulin sedimented (Fig. 1). Under such conditions, bovine tubulin was found predominantly in the pellet, as expected, but a shift to the supernatant was seen upon the addition of the MT disassembling agent vinblastine (79% of tubulin in supernatant: data not shown). When either MBP- α / β *P. falciparum* tubulin was centrifuged alone, it was absent from the pellet, but when mixed with bovine brain tubulin, the MBP- α / β tubulins were detected in the pellets. Altering the ratios of *P. falciparum* to bovine tubulin showed that the MBP-tubulin fusions were co-sedimented with bovine brain tubulin in a concentration-dependent fashion, presumably by being incorporated into growing MT. For MBP- β -tubulin to be capable of co-assembly it required pre-treatment with mercaptoethanol, indicating that some of its cysteine residues were possibly oxidised. Mercaptoethanol had little observable effect on MBP- α I-tubulin (data not shown). The control protein BSA did not demonstrate any co-sedimentation with bovine tubulin (Supplementary Fig. S1). We attempted to determine if the recombinant *Plasmodium* tubulin could displace the bovine brain monomers in the experiment shown in Fig. 1. The bovine brain tubulin monomers were separated into distinct bands by using a modified SDS-PAGE which had impure SDS and more basic buffers, a technique devised by Banerjee et al. [42]. Using densitometry, it was possible to determine that the relative concentrations of the tubulin monomers were similar, indicating that no detectable displacement had been caused by the presence of the recombinant tubulin (Supplementary Fig. S2).

Since the α / β tubulin dimer is the most physiologically relevant form of soluble (unassembled) tubulin, we wanted to carry out ligand binding studies using dimers, if possible. MBP- α I-tubulin or MBP alone were incubated in the presence or absence of MBP- β -tubulin-His₆ at 37 °C before being passed through a nickel-chelate column to determine whether they interacted. The tubulin or MBP that had not interacted with the MBP- β -tubulin-His₆ was readily washed off the column by a low imidazole concentration (60 mM). However, in the case of a real interaction, the protein would co-elute with MBP- β -tubulin-His₆ following the high imidazole concentration (500 mM) elution step. Only negligible amounts (<0.1 μ g) of MBP or MBP- α I-tubulin were recovered in the absence

resolved by SDS-10% PAGE and stained with Coomassie Blue. (D, I) Equal proportions from the supernatant (S) and pellet (P) fractions from experiments A and F respectively (MBP-tubulin + bovine tubulin) are shown. The extents of the MBP-tubulin incorporation into polymerised bovine brain tubulin for experiments A-C and F-H were quantified by densitometry (E and J respectively): X-axis values are concentrations of MBP-tubulin. The running positions of molecular weight markers are shown in kDa on the left of each gel. Upper arrows indicate MBP-tubulins and lower arrows bovine tubulins.

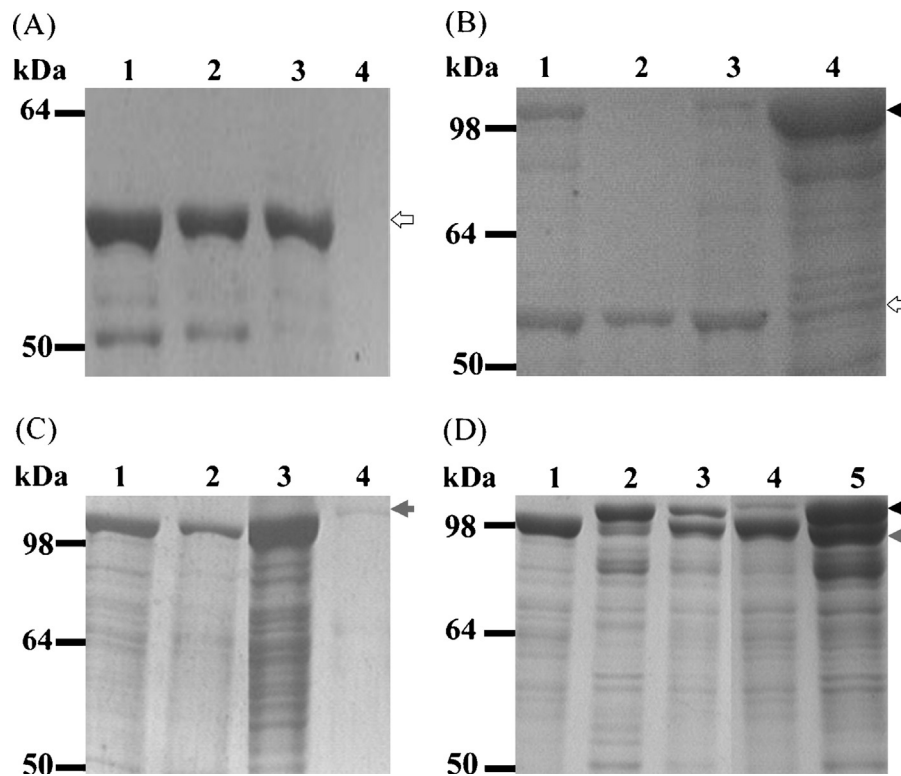


Fig. 2. Purification of the MBP-tubulin-His₆ by metal affinity chromatography after incubation with other tubulins or MBP. Proteins were separated by SDS-PAGE and stained with Coomassie Blue. (A) MBP incubated alone. (B) MBP-β-tubulin-His₆ and MBP incubated together. (C) MBP-α-tubulin incubated alone. For panels (A)–(C): (1) sample applied to the metal affinity column, (2) flow-through sample, (3) 60 mM imidazole wash sample and (4) 500 mM imidazole eluate. (D) MBP-β-tubulin-His₆ incubated with MBP-α-tubulin. (1) MBP-α-tubulin (5 μg), (2) MBP-β-tubulin-His₆ (5 μg), (3) sample applied to the metal affinity column, (4) 60 mM imidazole wash sample and (5) 500 mM imidazole eluate. The data shown are representative of experiments carried out in triplicate. White arrows indicate MBP, grey arrows indicate MBP-α-tubulin and black arrows indicate MBP-β-tubulin-His₆.

of MBP-β-His₆ tubulin as determined by densitometry (Fig. 2A and C). However, in its presence, there was an obvious band representing MBP-α-tubulin that was not present in the case of MBP alone (compare Fig. 2D and B). This indicated that MBP-α-tubulin is capable of specifically interacting with MBP-β-His₆ tubulin, suggesting that dimerisation is possible.

3.2. Validation of proposed herbicide binding sites in *P. falciparum* α-tubulin

α-Tubulin genes from a wide cross-section of herbicide-resistant and -sensitive organisms were aligned (Supplementary Fig. S3). This alignment highlights the amino acids comprising the three putative dinitroaniline herbicide binding sites of Mitra and Sept [36] from *Toxoplasma gondii*, Délye et al. [34] from green foxtail and Nyporko et al. [37] from *Eleusine indica*, and identifies the amino acid overlaps. Although the proposed binding sites are distinct, with only L136 common to them all, they were found to exist in the same region of the tubulin molecule. However, none of the amino acids predicted by any of the sites was unique to either resistant or sensitive organisms. In fact only half of all the amino acids that comprise the putative ‘Mitra & Sept’ site are completely conserved. Therefore we set about introducing amino acid changes that would be expected to occlude the sites, concentrating mainly on the ‘Mitra & Sept’ site due to the close relationship between *T. gondii* and *Plasmodium* [36]. Furthermore, there is more substantial experimental support for this site than for the ‘Délye’ or ‘Nyporko’ sites [34,37]. Six separate point mutations in the *P. falciparum* α-tubulin gene were chosen. *In silico* models were generated to demonstrate

that the altered residues were central to the sites and that they were expected dramatically to alter the structure of the putative binding pocket compared with the wild type protein (Fig. 3). The six altered MBP-α-tubulins were purified to near homogeneity with minimal degradation observed by either SDS-PAGE or western blotting (Supplementary Fig. S4).

To determine the affinity of the herbicides for the recombinant *P. falciparum* tubulins, a fluorescence assay was developed. Essentially, tubulin-ligand interactions were reported by the quenching of tryptophan fluorescence (Fig. 4A). A double reciprocal plot with the fluorescence reduction vs ligand concentration was graphed and from this it was possible to determine the dissociation constant (K_d) by using the formula described by Acharya et al. [45] (Fig. 4B). As a positive control, the K_d of vinblastine for bovine tubulin was determined to be $0.91 \pm 0.29 \mu\text{M}$, which was consistent with previous reports [51]. The MBP-tubulins were measured as monomers ($0.3 \mu\text{M}$) or as a 1:1 mixture of αI- and β-tubulins ($0.15 \mu\text{M}$ each). An equi-molar concentration of tryptophans was present in the samples to minimise error caused by using different tryptophan controls, which was the reason for using twice the molar concentration of the monomer compared with the mixture. At least five different ligand concentrations were used for determining the K_d . The phosphorothioamidate APM was able to quench the MBP-αI/β-tubulin mixture significantly over a range of concentrations (Fig. 4A). MBP-αI-tubulin had greater affinity for APM than MBP-β-tubulin but the mixture had the greatest affinity (Table 1A). Therefore, only the tubulin mixture was used for subsequent binding analysis. Oryzalin, a dinitroaniline, was demonstrated to bind with almost 3-fold higher affinity

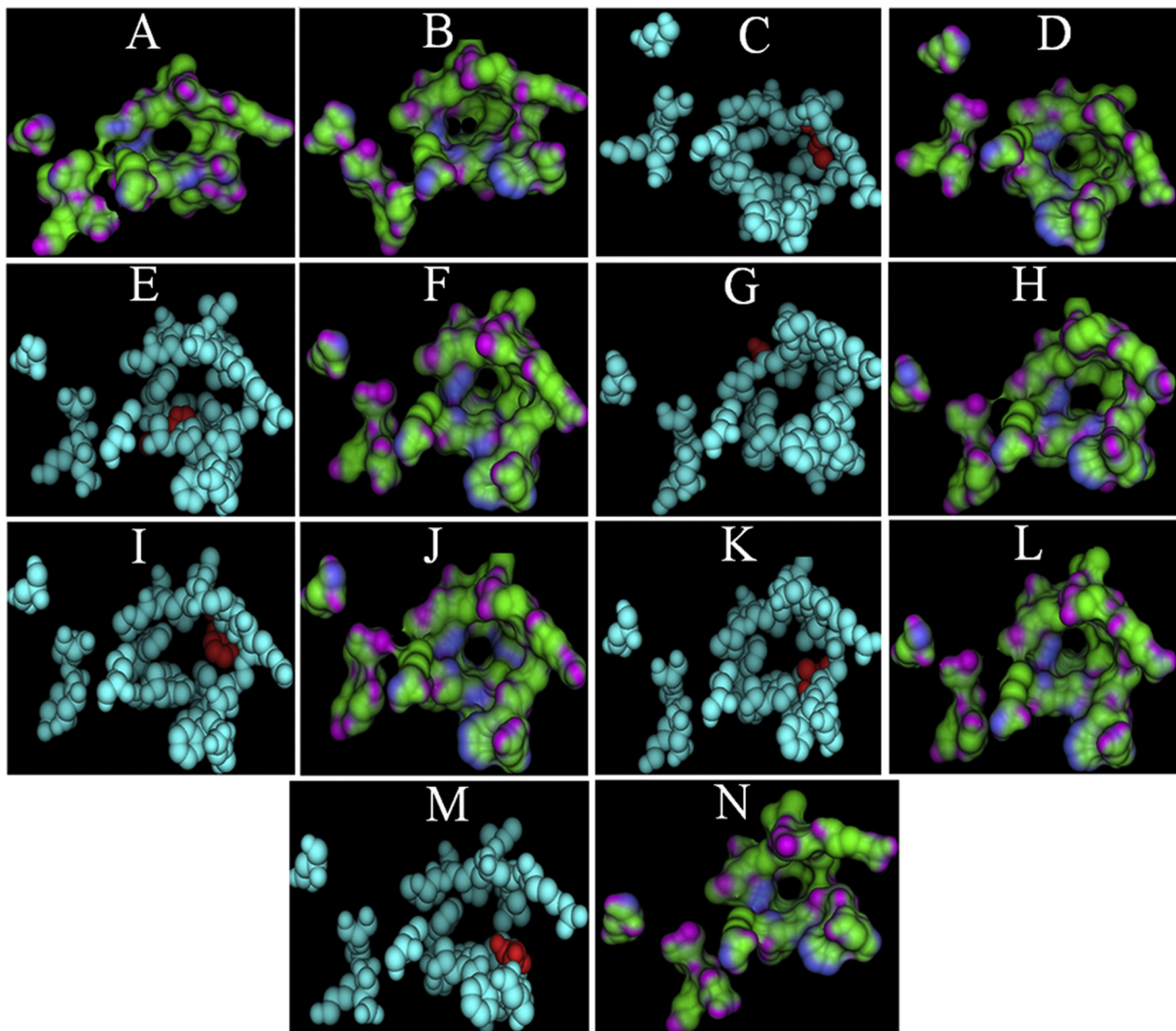


Fig. 3. Models of the putative 'Mitra & Sept' binding site on WT and altered *P. falciparum* α -tubulin. Only the 'Mitra & Sept' site is highlighted. The models were displayed using either a surface molecular map (Connolly analytic) (A, B, D, F, H, J, L and N) or space-filled amino acids (C, E, G, I, K and M). The surface molecular map highlights predicted hydrophobic (green), polar (blue) and hydrogen-bonding (purple) regions. The space-filled models highlight the 'Mitra & Sept' site residues (aqua) or the specific alteration (red). (A) *B. taurus* α -tubulin. (B) Homology model of the *P. falciparum* α -tubulin wild type; (C, D) Val4Cys alteration; (E, F), Phe24His alteration; (G, H), Cys65Ala alteration; (I, J) Leu136Phe alteration; (K, L) Thr239Ile alteration; (M, N) Arg243Ser alteration.

($15.51 \pm 3.55 \mu\text{M}$) to the MBP- α / β -tubulin mixture than APM ($44.14 \pm 7.15 \mu\text{M}$) (Table 1A). K_d values were also generated for each of the six altered tubulins (mixed 1:1 with MBP- β -tubulin) for both APM and oryzalin (Table 1B). Surprisingly, none of the mutations had the dramatic effect expected if the binding site had been occluded. For APM, the maximum increase in K_d relative to the wild type was a mere ~ 1.3 -fold and only 2/6 alterations (Cys65Ala and Thr238Ile) reached statistical significance. For oryzalin, the K_d increased by no more than 1.6-fold and of the five K_d determined only Val4Cys and Leu136Phe were significantly higher than the wild type. Taken together, these results cast doubt on the idea that the putative 'Mitra & Sept' binding site is applicable to *Plasmodium* tubulin. Regarding the 'Déllye' and 'Nyporko' sites, each of these should be occluded by 3 of the 6 mutations chosen so it also seems unlikely that either of these sites represents the actual location of herbicide binding in *Plasmodium* tubulin. It should be borne in mind however that these results were obtained with recombinant tubulins containing MBP tags.

3.3. Activity of herbicides against liver-stage malarial parasites

The activities of APM and oryzalin against *P. berghei* liver stages in culture were evaluated using established methods for measurement of infection loads in hepatoma cells [52]. Our results show that both compounds inhibit overall infection, as measured by bioluminescence readings of cells infected with luciferase-expressing parasites [46] with IC_{50} values of ~ 4.6 and $\sim 3.5 \mu\text{M}$, respectively (Fig. 5A). We further observed that both APM and oryzalin inhibited infection to similar extents whether they were added to the cells before infection or after the parasites had invaded the cells, suggesting that the compounds act by inhibiting intracellular parasite replication (data not shown). To verify this conclusion, we employed GFP-expressing *P. berghei* parasites and monitored the extent of their development by flow cytometry, as previously described [47]. These results show that incubation of both cells with either compound significantly decreases GFP fluorescence intensity of the infected cells ($p < 0.001$; Fig. 5B), confirming that the compounds act by impairing the parasite's ability to replicate

Table 1List of the binding affinities (K_d) for tubulin ligands of bovine brain tubulin and wild type MBP-tubulin fusions (A) or altered MBP-tubulin fusions (B).

(A)						
Tubulins	Conc (μM)	APM K_d (μM)	F_{max} R^2 value ^a			
MBP- α -tubulin	0.3	87.40 \pm 19.91	0.8852			
MBP- β -tubulin	0.3	162.63 \pm 24.72	0.9048			
MBP- α/β -tubulin	0.15	44.14 \pm 7.15	0.9712			
		Oryzalin K_d (μM)				
MBP- α/β -tubulin	0.15	15.51 \pm 3.55	0.9453			
		Vinblastine K_d (μM)				
Bovine brain tubulin	0.15	0.91 \pm 0.29 μM	0.8797			
(B)						
Tubulins	APM K_d (μM)	F_{max} R^2 value	p -Value ^b	Oryzalin K_d (μM)	F_{max} R^2 value	p -Value
α_{1V4C}/β	34.89 \pm 7.79	0.7457	0.1182	25.26 \pm 5.33	0.9995	0.004
α_{F24H}/β	47.28 \pm 9.88	0.9295	0.5555	15.31 \pm 4.36	0.8261	0.9313
α_{C65A}/β	57.27 \pm 8.10	0.9709	0.0106	13.75 \pm 1.96	0.9955	0.2819
α_{L136F}/β	46.52 \pm 17.54	0.9869	0.7665	24.56 \pm 7.54	0.9581	0.0239
α_{T239I}/β	57.95 \pm 6.01	0.9203	0.0076	N.D. ^c	N.D.	N.D.
α_{R243S}/β	32.49 \pm 12.36	0.925	0.0676	17.64 \pm 4.51	0.9345	0.372

^a F_{max} R^2 value, the correlation co-efficient of the line measuring the F_{max} (F_{max} = maximum possible quench if the ligand the ligand occupies all of its binding sites on tubulin).

^b The p values shown were obtained using the Student t test and refer to the difference between the wild type and altered tubulin(s).

^c Not determined.

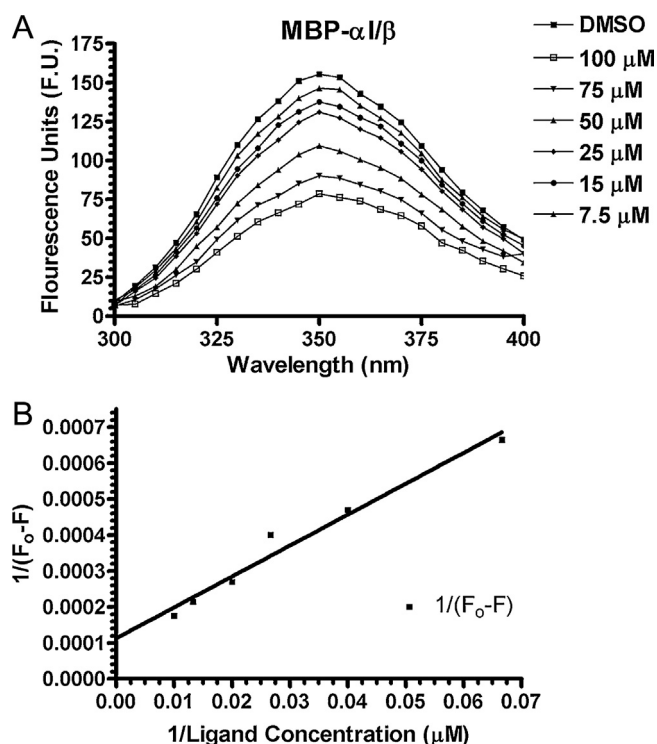


Fig. 4. Analysis of the intrinsic fluorescence of MBP- α/β -tubulin mixture in the presence of different concentrations of APM. (A) The MBP- α/β -tubulin mixture (0.15 μM) was incubated with either DMSO (control) or different concentrations of APM as indicated for 5 min at 37 $^{\circ}\text{C}$. Three independent samples were used for each concentration. For reasons of clarity, the error bars have been omitted and the uncorrected fluorescence was graphed. (B) Double reciprocal plot of the corrected fluorescence change and ligand concentration. A best fit line was used to plot the graph (R^2 value = 0.9712). The F_{max} (the point of interception at the Y-axis) was used to predict the maximum fluorescence quench achievable. F_0 represents the observed fluorescence in the absence of a ligand (after correction). F represents the observed fluorescence in the presence of a ligand (after correction).

inside its host cells. Finally, we sought to investigate the effect of the two compounds on the microtubular network of liver stage *Plasmodium* parasites. To this end, infected cells incubated with each compound or mock-treated with solvent were stained using an

antibody against the parasite's MT and observed by confocal fluorescence microscopy. These observations indicated that treatment with either compound disrupted the filamentous microtubular pattern inside the parasite (Fig. 5C), consistent with both inhibitors interfering with normal tubulin assembly and, hence, parasite replication. Overall, our data are consistent with the notion that the two herbicides used in this study inhibit hepatic stage *Plasmodium* infection by acting on the parasites' microtubular structures to impair their development/replication inside host cells.

4. Discussion

The recent emergence of malarial parasites with reduced artemisinin susceptibility [53] underlines the still urgent need to identify new drug targets in and new lead compounds against the disease-associated, asexual blood-stage malarial parasites. In addition, primaquine is the only licensed drug for the liver stages of the disease and it suffers from drawbacks in terms of toxicity [11]. Antimitotic herbicides of the dinitroaniline and phosphorothioamide classes offer potential starting points for the design of new drugs targeting MT-dependent processes in malarial parasites [54]. In this study we have extended previous observations on blood-stage parasites to those of the liver stage of the rodent parasite *P. berghei*. We observed that the two compounds assayed in this study, APM and oryzalin, inhibited *Plasmodium* hepatic infection with single-digit micromolar IC_{50} values comparable to those on blood stages [7] and lower than that of primaquine ($\sim 11 \mu\text{M}$) measured by the same method [46]. We further established that the compounds disrupted the microtubular network of the exoerythrocytic parasite. It appears that MT inhibitors may be a promising class of agents for liver-stage malaria.

While the dinitroaniline herbicides themselves had unsuitable pharmacokinetics and/or toxicity in rodent malaria models [55], numerous more drug-like derivatives have been reported [4,56]. None of these was superior to the dinitroanilines themselves against *Plasmodium*, but Mara et al. [54] recently achieved modest reductions in IC_{50} against cultured *P. falciparum* in some members of a series of compounds related to APM. Greater improvements in activity have been obtained against trypanosomes [27] and *Leishmania* spp. [56] but these protozoa are quite unrelated to *Plasmodium* and their structure-activity relationships are apparently very different.

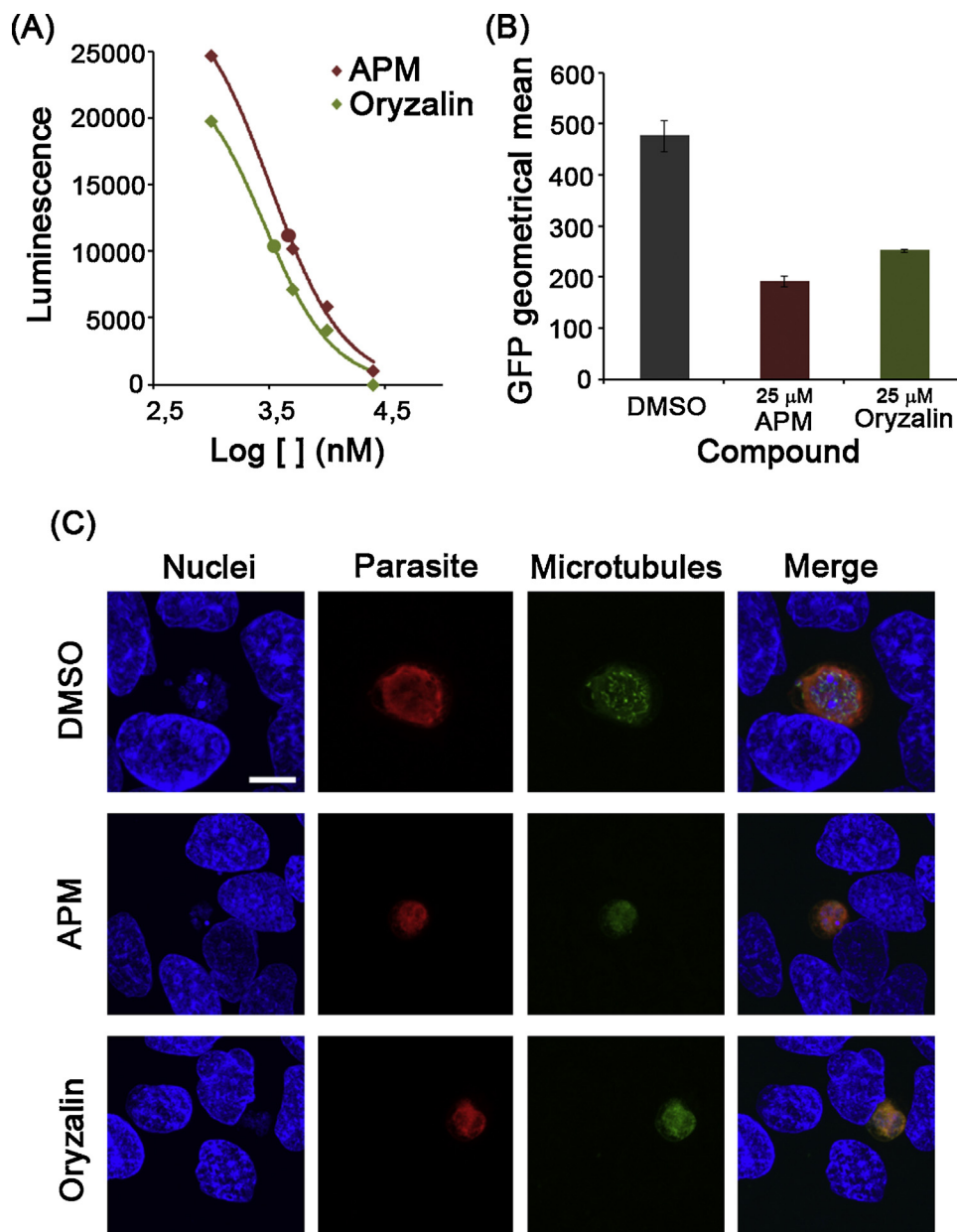


Fig. 5. Activity of herbicides against *Plasmodium* liver stages. (A) Sigmoidal inhibition curves and IC_{50} determination for APM (red) and oryzalin (green). Huh7 cells were infected with luciferase-expressing *P. berghei* sporozoites and incubated with 1, 5, 10 or 25 μ M of each compound for 48 h, prior to measurement of parasite load by bioluminescence. (B) Effect of 25 μ M APM (red) and 10 μ M oryzalin (green) on parasite development. The geometrical mean of the GFP intensity of Huh7 cells 48 h after infection with GFP-expressing *P. berghei* sporozoites is a measure of the extent of parasite replication [47]. Vertical bars show standard errors. (C) Representative maximum intensity projections of confocal fluorescence microscopy images of *P. berghei*-infected Huh7 cells. Cells were solvent-treated or treated with 25 μ M APM or 10 μ M oryzalin, fixed 48 h after infection, and stained for *Plasmodium* Hsp70 (red), β -tubulin (green), and nuclei (blue). The scale bar in the top left panel applies at all panels and corresponds to 10 μ m.

A significant barrier to structure-based drug design based on this theme is the lack of a known 3D structure for any tubulin of a herbicide-susceptible organism. This necessitates modelling of plant and protozoal tubulins using mammalian tubulins as a template, yet the mammalian tubulins evidently lack the site [4]. The three modelled herbicide-binding sites proposed in the literature [33–37] must therefore be treated with some scepticism. A notable exception has been the recent work by Lyons-Abbott et al. who demonstrated that Leu136Phe and Ile252Leu mutations affect binding of oryzalin to *Tetrahymena* α -tubulin [38].

In order to validate the proposed herbicide-binding sites in *Plasmodium* tubulin and to evaluate the binding affinities of novel herbicide derivatives, we required a reasonably abundant source

of soluble parasite tubulins. To date, it has not been possible to isolate tubulin directly from *Plasmodium* due to the limited amounts of starting material and low concentrations of tubulin in cultured parasites (~ 0.1 mg/l in a culture of 10% parasitaemia and 5% haematocrit). Therefore, we opted for a recombinant strategy using *E. coli* as a host. While lacking the post-translational modifications expected in eukaryotic cells, tubulins produced in this way have the advantages of lack of intrinsic tubulin contamination, high protein yields and freedom to alter the tubulin gene in a way that could be lethal for a eukaryotic cell. Tubulins from several other organisms produced in *E. coli* have been shown to bind small-molecule ligands and antibodies and in some cases to dimerise and even to assemble into MT [7,18–27,30].

Several groups have argued that tubulin requires specific machinery in order to fold correctly [57–59] but other reports demonstrated MT formation by isolated recombinant tubulins [21,26,28,60,61]. Success using this method seems to depend on the source of the tubulin, and subtle but significant differences between these proteins may explain the disparity. Bacterial tubulins have been recently discovered in some *Prostheco bacter* species, and recombinant proteins made in *E. coli* formed functional MT [62]. In our case, following extensive investigation of various expression systems the only one that produced useful quantities of soluble *P. falciparum* tubulins was one in which the tubulins were fused to MBP tags [7]. The exact reason why the MBP tag causes an improvement to the solubility of the passenger protein is unknown [23] but MBP is thought to act as a general molecular chaperone [63]. A previous study by Yaffe et al. determined that an α -tubulin monomer can be stable without its partner protein β -tubulin but it was also capable of interacting with other preformed dimers in a co-polymerisation assay [50]. Since the MBP-tubulins described in the present study could not polymerise in the absence of other proteins, we determined that they could be incorporated into bovine MT, as shown by dose-dependent co-sedimentation with bovine tubulins after incubation under assembly promoting conditions. These results were specific as they were not replicated by unrelated proteins such as MBP or BSA. The exact mechanism for the incorporation of our MBP-tubulins into the bovine MT is unclear. Yaffe et al. argued that their refolded α -tubulin formed heterodimers [50]. However, in our case, we think this is unlikely. We separated the bovine tubulin that had bound to our MBP- α -tubulin and MBP- β -tubulin into its monomers and determined that they were in approximately equal concentration, indicating that no major displacement had occurred. Instead we propose that the MBP-tubulins would probably bind at the extreme ends of the MT's so that a partner protein would not be required for the interaction to occur. Binding here may also limit the steric hindrance effect that the MBP tag may have on the overall structure. Another possibility is that the MBP-tubulins are incorporated at low frequency along the shaft of the MT. It was also possible to demonstrate that the monomers had a significant affinity for each other over other unrelated proteins by their co-eluting after being trapped on a Ni^{2+} -chelate column. We have not been able to show that 100% of our MBP-tubulin molecules are correctly folded. However, Wampande et al. managed successfully to calculate binding affinities for native and chemically refolded tubulin [31]. They determined that although the native tubulin had lower K_d , the binding capacity and the rank order of affinity for several different ligands were the same [31]. Taken together, the results suggested that the MBP-tubulins had the potential to be useful for ligand-binding studies provided that the affinities obtained were comparable with those in the literature.

It was previously shown that radiolabelled trifluralin had much greater binding to purified tubulin from *Plasmodium* than that of bovine brain but an exact measurement of affinity was not obtained [7]. We addressed this issue here by using intrinsic tryptophan fluorescence to detect perturbations of the tubulin protein by small ligands such as the herbicides APM and oryzalin. We found that APM was able to bind to both monomers, but with ~ 2 -fold greater affinity to MBP- α -tubulin than to MBP- β -tubulin, indicating that the binding site may exist on both tubulins. This result has been reported before in the literature for other herbicide-based compounds [7,27,37]. However, we found that our α/β -tubulin mixture had the strongest affinity for APM. Furthermore, we found that oryzalin had almost a 3-fold greater affinity than APM for our tubulin, with a K_d of $15.51 \pm 3.55 \mu\text{M}$. The affinity of oryzalin has been examined using a range of diverse organisms and reported binding affinities range from $0.1 \mu\text{M}$ for plant tubulin to $17 \mu\text{M}$ for

Leishmania tubulin [64,65]. Therefore, our results fit closely with the recorded affinity for this ligand albeit at the higher end of the scale. This is not surprising as *Plasmodium* in culture is susceptible to this compound only in the low micromolar range and above (IC_{50} $6.1 \mu\text{M}$). APM is a slightly more potent inhibitor than oryzalin against cultured parasites (IC_{50} $3.5 \mu\text{M}$), perhaps because oryzalin, like trifluralin, may be more susceptible to sequestration in cell membranes [66]. This is the first time the interaction between small ligands and *Plasmodium* tubulin has been quantified.

Currently, at least three overlapping but distinct putative herbicide-binding sites, all of which reside on α -tubulin, have been proposed [34–37]. To date, there have been no *in vitro* ligand-tubulin binding or any other data demonstrating that any of them applies to *Plasmodium*. However, Mitra and Sept have argued that their refined site can be modelled in *Plasmodium* tubulin so we focused primarily on it [36]. We altered 6 different residues on α -tubulin based on amino acids that lined the proposed binding pocket but also on previously generated mutations [67]. To confirm that our alterations would prevent or substantially reduce binding, we made molecular models of all the changes to ensure that they would be central in the 'Mitra & Sept' site on *Plasmodium* tubulin. However, for neither APM nor oryzalin were substantial decreases in binding affinity, compared with wild type, apparent. The small changes observed for some alterations were probably due to slight allosteric effects. These results are in contrast to previous work that demonstrated that L136F was responsible for almost 20-fold decreased binding of oryzalin to the mutated tubulin [38]. There are several possible explanations for this incongruity. Our recombinant tubulins may not be forming the correct binding pocket owing to improper folding. We think this possible but unlikely, based on the functional characterisation reported here and in Fennell et al. [7] and the fact that the K_d values for the wild-type tubulins are in line with previous reports from other species. Another possibility is that the 'Mitra & Sept' site may be present in *T. gondii* but not in *Plasmodium*. *T. gondii* cultures are approximately 10-fold more sensitive to oryzalin than *Plasmodium* [7,68] and this may be illustrative of different binding affinities of this ligand to the tubulin from these two organisms. The existence in such a highly conserved protein of two or more distinct sites among α -tubulins of the herbicide-susceptible organisms, but absent from those of the herbicide-resistant ones, seems however an unlikely prospect. Even if this were so, one might expect two organisms as closely related as *Plasmodium* and *Toxoplasma* to share the same site. A third possibility, and the one we consider most probable, is that the level of sophistication of molecular modelling does not yet permit sufficiently accurate estimation of the structure of the herbicide-binding site, given that it by definition lies outside the region of sequence identity with the template (mammalian) tubulin. In this case, while it may be in the general area highlighted by the 'Mitra & Sept', 'Délye' and 'Nyporko' sites, the exact location and architecture of the binding pocket still remains to be determined. Obtaining this information may open the door to structure-based approaches to new, potent and selective antimalarial MT inhibitors active on both blood- and liver-stage parasites.

Acknowledgements

This work was supported by grants from the Enterprise Ireland Commercialisation Fund (no. PC/2005/0700) to AB and JW, the Irish Research Council for Science, Engineering and Technology to BJF and AB, Science Foundation Ireland (no. 08/BMT/1062) to AB, and Fundação para a Ciência e Tecnologia, Portugal (nos. PTDC/SAU-MII/099118/2008 and PTDC/SAU-MIC/117060/2010) to MP.

Appendix A. Supplementary data

Supplementary data associated with this article can be found, in the online version, at <http://dx.doi.org/10.1016/j.molbiopara.2013.03.001>.

References

- [1] Wade RH. Microtubules: an overview. *Methods in Molecular Medicine* 2007;137:1–16.
- [2] Jordan MA, Kamath K. How do microtubule-targeted drugs work? An overview. *Current Cancer Drug Targets* 2007;7:730–42.
- [3] Wilson L, Jordan MA. New microtubule/tubulin-targeted anticancer drugs and novel chemotherapeutic strategies. *Journal of Chemotherapy* 2004;16(Suppl. 4):83–5.
- [4] Fennell BJ, Naughton JA, Barlow J, Brennan G, Fairweather I, Hoey E, et al. Microtubules as antiparasitic drug targets. *Expert Opinion on Drug Discovery* 2008;3:501–18.
- [5] Chatterji BP, Jindal B, Srivastava S, Panda D. Microtubules as antifungal and antiparasitic drug targets. *Expert Opinion on Therapeutic Patents* 2011;21:167–86.
- [6] Fennell BJ, Carolan S, Pettit GR, Bell A. Effects of the antimitotic natural product dolastatin 10, and related peptides, on the human malarial parasite *Plasmodium falciparum*. *Journal of Antimicrobial Chemotherapy* 2003;51:833–41.
- [7] Fennell BJ, Naughton JA, Dempsey E, Bell A. Cellular and molecular actions of dinitroaniline and phosphorothioamidate herbicides on *Plasmodium falciparum*: tubulin as a specific antimalarial target. *Molecular and Biochemical Parasitology* 2006;145:226–38.
- [8] Pinder J, Fowler R, Bannister L, Dluzewski A, Mitchell GH. Motile systems in malaria merozoites: how is the red blood cell invaded? *Parasitology Today* 2000;16:240–5.
- [9] Bell A. Microtubule inhibitors as potential antimalarial agents. *Parasitology Today* 1998;14:234–40.
- [10] Rodrigues T, Prudencio M, Moreira R, Mota MM, Lopes F. Targeting the liver stage of malaria parasites: a yet unmet goal. *Journal of Medicinal Chemistry* 2012;55:995–1012.
- [11] Derbyshire ER, Mota MM, Clardy J. The next opportunity in anti-malaria drug discovery: the liver stage. *PLoS Pathogens* 2011;7:e1002178.
- [12] Kappes B, Rohrbach P. Microtubule inhibitors as a potential treatment for malaria. *Future Microbiology* 2007;2:409–23.
- [13] Morejohn LC, Fosket DE. The biochemistry of compounds with anti-microtubule activity in plant cells. *Pharmacology & Therapeutics* 1991;51:217–30.
- [14] Traub-Cseko YM, Ramalho-Ortigao JM, Dantas AP, de Castro SL, Barbosa HS, Downing KH. Dinitroaniline herbicides against protozoan parasites: the case of *Trypanosoma cruzi*. *Trends in Parasitology* 2001;17:136–41.
- [15] Anthony RG, Hussey PJ. Double mutation in *Eleusine indica* alpha-tubulin increases the resistance of transgenic maize calli to dinitroaniline phosphorothioamidate herbicides. *Plant Journal* 1999;18:669–74.
- [16] Smith JA, Jordan MA. Determination of drug binding to microtubules in vitro. *Methods in Cell Biology* 2010;95:289–99.
- [17] Sackett DL, Werbovetz KA, Morrissette NS. Isolating tubulin from nonneural sources. *Methods in Cell Biology* 2010;95:17–32.
- [18] Lubega GW, Geary TG, Klein RD, Prichard RK. Expression of cloned beta-tubulin genes of *Haemonchus contortus* in *Escherichia coli*: interaction of recombinant beta-tubulin with native tubulin and mebendazole. *Molecular and Biochemical Parasitology* 1993;62:281–92.
- [19] Hollomon DW, Butters JA, Barker H, Hall L. Fungal beta-tubulin, expressed as a fusion protein, binds benzimidazole and phenylcarbamate fungicides. *Antimicrobial Agents and Chemotherapy* 1998;42:2171–3.
- [20] Linder S, Schliwa M, Kube-Granderath E. Expression of Reticulomyxa filosa alpha- and beta-tubulins in *Escherichia coli* yields soluble and partially correctly folded material. *Gene* 1998;212:87–94.
- [21] Oxberry ME, Gear TG, Prichard RK. Assessment of benzimidazole binding to individual recombinant tubulin isotypes from *Haemonchus contortus*. *Parasitology* 2001;122:683–7.
- [22] MacDonald LM, Armson A, Thompson AR, Reynoldson JA. Characterisation of benzimidazole binding with recombinant tubulin from *Giardia duodenalis*, *Encephalitozoon intestinalis*, and *Cryptosporidium parvum*. *Molecular and Biochemical Parasitology* 2004;138:89–96.
- [23] MacDonald LM, Armson A, Thompson RC, Reynoldson JA. Characterization of factors favoring the expression of soluble protozoan tubulin proteins in *Escherichia coli*. *Protein Expression and Purification* 2003;29:117–22.
- [24] MacDonald LM, Armson A, Thompson RC, Reynoldson JA. Expression of *Giardia duodenalis* beta-tubulin as a soluble protein in *Escherichia coli*. *Protein Expression and Purification* 2001;22:25–30.
- [25] Pucciarelli S, Miceli C, Melki R. Heterologous expression and folding analysis of a beta-tubulin isotype from the Antarctic ciliate *Euplotes focardii*. *European Journal of Biochemistry* 2002;269:6271–7.
- [26] Jang MH, Kim J, Kalme S, Han JW, Yoo HS, Koo BS, et al. Cloning, purification, and polymerization of *Capsicum annuum* recombinant alpha and beta tubulin. *Bioscience, Biotechnology, and Biochemistry* 2008;72:1048–55.
- [27] Giles NL, Armson A, Reid SA. Characterization of trifluralin binding with recombinant tubulin from *Trypanosoma brucei*. *Parasitology Research* 2009;104:893–903.
- [28] Oxberry ME, Geary TG, Winterrowd CA, Prichard RK. Individual expression of recombinant alpha- and beta-tubulin from *Haemonchus contortus*: polymerization and drug effects. *Protein Expression and Purification* 2001;21:30–9.
- [29] Beghin A, Galmarini CM, Dumontet C. Tubulin folding pathways: implication in the regulation of microtubule dynamics. *Current Cancer Drug Targets* 2007;7:697–703.
- [30] Shah C, Xu CZ, Vickers J, Williams R. Properties of microtubules assembled from mammalian tubulin synthesized in *Escherichia coli*. *Biochemistry* 2001;40:4844–52.
- [31] Wampande EM, Richard McIntosh J, Lubega GW. Classical ligands interact with native and recombinant tubulin from *Onchocerca volvulus* with similar rank order of magnitude. *Protein Expression and Purification* 2007;55:236–45.
- [32] Chambers E, Ryan LA, Hoey EM, Trudgett A, McFerran NV, Wilbur N, et al. Liver fluke beta-tubulin isotype 2 binds albendazole and is thus a probable target of this drug. *Parasitology Research* 2010;107:1257–64.
- [33] Blume YB, Nyporko AY, Yemets AI, Baird FFV. Structural modeling of the interaction of plant alpha-tubulin with dinitroaniline and phosphoramidate herbicides. *Cell Biology International* 2003;27:171–4.
- [34] Delye C, Menchari Y, Michel S, Darmency H. Molecular bases for sensitivity to tubulin-binding herbicides in green foxtail. *Plant Physiology* 2004;136:3920–32.
- [35] Morrissette NS, Mitra A, Sept D, Sibley LD. Dinitroanilines bind alpha-tubulin to disrupt microtubules. *Molecular Biology of the Cell* 2004;15:1960–8.
- [36] Mitra A, Sept D. Binding and interaction of dinitroanilines with apicomplexan and kinetoplastid alpha-tubulin. *Journal of Medicinal Chemistry* 2006;49:5226–31.
- [37] Nyporko A, Emets AI, Brytsun VN, Lozinskii MO, Blum Ia B. Structural-biological characteristics of tubulin interaction with dinitroanilines. *Tsitol Genet* 2009;43:56–70.
- [38] Lyons-Abbott S, Sackett DL, Wloga D, Gaertig J, Morgan RE, Werbovetz KA, et al. α -Tubulin mutations alter oryzalin affinity and microtubule assembly properties to confer dinitroaniline resistance. *Eukaryotic Cell* 2010;9:1825–34.
- [39] Maniatis T, Fritsch E, Sambrook J. *Molecular cloning: a laboratory manual*. New York: Cold Spring Harbour; 1982.
- [40] Kumar N. Taxol-induced polymerization of purified tubulin. Mechanism of action. *The Journal of Biological Chemistry* 1981;256:10435–41.
- [41] Bell A, Wernli B, Franklin RM. Expression and secretion of malarial parasite beta-tubulin in *Bacillus brevis*. *Biochimie* 1995;77:256–61.
- [42] Banerjee A, Bovenzi FA, Bane SL. High-resolution separation of tubulin monomers on polyacrylamide minigels. *Analytical Biochemistry* 2010;402:194–6.
- [43] Nogales E, Wolf SG, Downing KH. Structure of the alpha beta tubulin dimer by electron crystallography. *Nature* 1998;391:199–203.
- [44] Lakowicz JR. *Principles of fluorescence spectroscopy*. New York: Kluwer Academic/Plenum Publishers; 1999.
- [45] Acharya BR, Bhattacharyya B, Chakrabarti G. The natural naphthoquinone plumbagin exhibits antiproliferative activity and disrupts the microtubule network through tubulin binding. *Biochemistry* 2008;47:7838–45.
- [46] Ploemen IH, Prudencio M, Douradinha BG, Ramesar J, Fonager J, van Gemert GJ, et al. Visualisation and quantitative analysis of the rodent malaria liver stage by real time imaging. *PLoS ONE* 2009;4:e7881.
- [47] Prudencio M, Rodrigues CD, Ataide R, Mota MM. Dissecting in vitro host cell infection by *Plasmodium sporozoites* using flow cytometry. *Cellular Microbiology* 2008;10:218–24.
- [48] Prescott AR, Foster KE, Warn RM, Gull K. Incorporation of tubulin from an evolutionarily diverse source *Physarum polycephalum*, into the microtubules of a mammalian cell. *Journal of Cell Science* 1989;92(4):595–605.
- [49] Phadtare S, Fisher MT, Yarbrough LR. Refolding and release of tubulins by a functional immobilized groEL column. *Biochimica et Biophysica Acta* 1994;1208:189–92.
- [50] Yaffe MB, Levison BS, Szasz J, Sternlicht H. Expression of a human alpha-tubulin: properties of the isolated subunit. *Biochemistry* 1988;27:1869–80.
- [51] Avila J. *Microtubule proteins*. CRC Press; 1990:1–270.
- [52] Prudencio M, Mota MM, Mendes AM. A toolbox to study liver stage malaria. *Trends in Parasitology* 2011;27:565–74.
- [53] Dondorp AM, Yeung S, White L, Nguon C, Day NP, Socheat D, et al. Artemisinin resistance: current status and scenarios for containment. *Nature Reviews Microbiology* 2010;8:272–80.
- [54] Mara C, Dempsey E, Bell A, Barlow JW. Synthesis and evaluation of phosphoramidate and phosphorothioamidate analogues of amiprophos methyl as potential antimalarial agents. *Bioorganic & Medicinal Chemistry Letters* 2011;21:6180–3.
- [55] Dow GS, Armson A, Boddy MR, Itenge T, McCarthy D, Parkin JE, et al. Plasmodium: assessment of the antimalarial potential of trifluralin and related compounds using a rat model of malaria, *Rattus norvegicus*. *Experimental Parasitology* 2002;100:155–60.
- [56] Werbovetz KA, Sackett DL, Delfin D, Bhattacharyya G, Salem M, Obrzut T, et al. Selective antimicrotubule activity of N1-phenyl-3,5-dinitro-N4,N4-di-n-propylsulfanilamide (GB-II-5) against kinetoplastid parasite. *Molecular Pharmacology* 2003;64:1325–33.
- [57] Guha S, Bhattacharyya B. Refolding of urea-denatured tubulin: recovery of natively like structure and colchicine binding activity from partly unfolded states. *Biochemistry* 1997;36:13208–13.

- [58] Llorca O, Martin-Benito J, Ritco-Vonsovici M, Grantham J, Hynes GM, Willison KR, et al. stabilizes actin tubulin folding intermediates in open quasi-native conformations. *EMBO Journal* 2000;19:5971–9.
- [59] Lewis SA, Tian G, Cowan NJ. The alpha- and beta-tubulin folding pathways. *Trends in Cell Biology* 1997;7:479–84.
- [60] Koo BS, Kalme S, Yeo SH, Lee SJ, Yoon MY. Molecular cloning and biochemical characterization of alpha- and beta-tubulin from potato plants (*Solanum tuberosum* L.). *Plant Physiology and Biochemistry* 2009;47:761–8.
- [61] Koo BS, Park H, Kalme S, Park HY, Han JW, Yeo YS, et al. Alpha- and beta-tubulin from *Phytophthora capsici* KACC 40483 molecular cloning, biochemical characterization, and antimicrotubule screening. *Applied Microbiology and Biotechnology* 2009;82:513–24.
- [62] Pilhofer M, Ladinsky MS, McDowall AW, Petroni G, Jensen GJ. Microtubules in bacteria: ancient tubulins build a five-protofilament homolog of the eukaryotic cytoskeleton. *PLoS Biology* 2011;9:e1001213.
- [63] Kapust RB, Waugh DS. Escherichia coli maltose-binding protein is uncommonly effective at promoting the solubility of polypeptides to which it is fused. *Protein Science* 1999;8:1668–74.
- [64] Murthy JV, Kim HH, Hanesworth VR, Hugdahl JD, Morejohn LC. Competitive inhibition of high-affinity oryzalin binding to plant tubulin by the phosphoric amide herbicide amiprofos-methyl. *Plant Physiology* 1994;105:309–20.
- [65] Yakovich AJ, Ragone FL, Alfonzo JD, Sackett DL, Werbovetz KA. Leishmania tarentolae: purification and characterization of tubulin and its suitability for antileishmanial drug screening. *Experimental Parasitology* 2006;114:289–96.
- [66] Naughton JA, Hughes R, Bray P, Bell A. Accumulation of the antimalarial microtubule inhibitors trifluralin and vinblastine by *Plasmodium falciparum*. *Biochemical Pharmacology* 2008;75:1580–7.
- [67] Ma C, Li C, Ganesan L, Oak J, Tsai S, Sept D, et al. Mutations in alpha-tubulin confer dinitroaniline resistance at a cost to microtubule function. *Molecular Biology of the Cell* 2007;18:4711–20.
- [68] Stokkermans TJ, Schwartzman JD, Keenan K, Morrissette NS, Tilney LG, Roos DS. Inhibition of *Toxoplasma gondii* replication by dinitroaniline herbicides. *Experimental Parasitology* 1996;84:355–70.